



Article

# Reduction of Cd(II) Ions in the Presence of Tetraethylammonium Cations. Adsorption Effect on the Electrode Process

Juan Torrent-Burgués

Department of Chemical Engineering, Universitat Politècnica de Catalunya (UPC), 08222 Barcelona, Spain; juan.torrent@upc.edu

**Abstract:** The effect of the adsorption of tetraethylammonium (TEA) cations, which present both ionic and organic characteristics, on the reduction of Cd(II) ions have been studied from dc and ac measurements at the dropping mercury electrode. The resistance to the charge transfer ( $R_{ct}$ ) and Warburg coefficient ( $\sigma$ ) parameters have been determined through impedance measurements. Thus, the global velocity constant has been obtained. The reduction process of Cd(II) in perchloric media is reversible and is affected by the adsorption of TEA cations, especially at high TEA concentrations. Values of  $E_{1/2}$ , half wave potential, and  $D_O$ , diffusion coefficient, obtained from both dc and ac measurements agree. The velocity constants show a decrease as TEA concentration increases, with values ranging from 0.6 to 0.01  $\text{cm}\cdot\text{s}^{-1}$ . The inhibitory effect of TEA adsorption on the electrode process and the relationship between electrode coverage,  $\theta$ , and velocity constants,  $K$ , using several isotherm equations, have been discussed. The best fit was obtained with the equation  $K = {}_0K(1 - \theta)^a$  with an  $a$  value close to three, indicating a blocking effect and electrostatic repulsion due to TEA.

**Keywords:** dropping mercury electrode (DME); tetraethylammonium cation (TEA); electrochemical impedance; electrochemical reduction of Cd(II); Randles circuit; adsorption of TEA; adsorption isotherm



**Citation:** Torrent-Burgués, J. Reduction of Cd(II) Ions in the Presence of Tetraethylammonium Cations. Adsorption Effect on the Electrode Process. *Electrochem* **2021**, *2*, 415–426. <https://doi.org/10.3390/electrochem2030027>

Academic Editor: Masato Sone

Received: 22 June 2021

Accepted: 19 July 2021

Published: 23 July 2021

**Publisher's Note:** MDPI stays neutral with regard to jurisdictional claims in published maps and institutional affiliations.



**Copyright:** © 2021 by the author. Licensee MDPI, Basel, Switzerland. This article is an open access article distributed under the terms and conditions of the Creative Commons Attribution (CC BY) license (<https://creativecommons.org/licenses/by/4.0/>).

## 1. Introduction

The reduction of Cd(II) ions at the dropping mercury electrode (DME) has been widely used to test models for electrode reactions. Nowadays, some characteristics of the process seem well established, as the CEE mechanism (C: chemical reaction, E: electron transfer) [1–4], but other questions remain unsolved when adsorption or complexation is present [5–9]. The catalytic effect or inhibition by organic substances could introduce changes in the mechanism or only influence values of the parameters and velocity constants. Particularly, the catalytic effect of thiourea has been studied [5,6], and it was concluded that thiourea adsorption changes the mechanism of Cd(II) reduction; however, the inhibition effect of sucrose [8] only influence the values of the velocity constants but the CEE mechanism remains. It seems interesting to study the effect of other adsorbing substances. Tetraethylammonium (TEA) ions have been selected because of their double character of ionic and organic, and because their adsorption has been studied previously [10,11]. TEA was selected formerly due to it be an organic cation but with an organic character in between that of TMA and TBA. TMA exhibits a behavior somewhat similar to an inorganic cation with a weak specific adsorption [12–15]. On the other hand, TBA presents a high organic character with a high specific adsorption, which induces a high adsorption of the salt anion [16]. In a previous polarographic study of the Eu(III)/Eu(II) reduction in the presence of TEA [11,17], both surface blocking and electrostatic interaction effects between the adsorbate and the electroactive ions were observed.

In this paper, the reduction of Cd(II) in the presence of TEA in a perchloric acid medium is presented, using dc and ac measurements. The activity of the perchloric acid was maintained constant [10,18,19] in order to apply a correct thermodynamic treatment. The adsorption results, obtained previously, are related to the electrode kinetic values

obtained in the present study. This study is a recognition to the notable contribution of Profs J.H. Sluyters and M. Sluyters-Rehbach and their group of the Van't Hoff Laboratory—University of Utrecht, and also a posthumous tribute to Prof F. Sanz, my PhD thesis supervisor, who introduced me to the electrochemical research field.

## 2. Theory

### 2.1. Polarograms

The equations that apply for the current intensity versus potential,  $i - E$ , in polarography are [20] the Ilkovic equation for the limit diffusion current (Equation (1)) with sphericity correction (Equation (2)), where  $i_d$  is the limit current intensity,  $D$  is the diffusion coefficient,  $m$  is the drop mass and  $t$  is the drop time.

$$i_d = 708ncD^{1/2}m^{2/3}t^{1/6} \quad (1)$$

$$i_d = 708ncD^{1/2}m^{2/3}t^{1/6}(1 + 39.7D^{1/2}t^{1/6}/m^{1/3}) \quad (2)$$

Equations (1) and (2) enable the calculation  $D$  once the other parameters are known.

The slope of  $\log(i/(i_d - i))$  vs.  $E$  (see Equation (3)) enables testing of the reversibility of the process and to obtain the half wave potential,  $E_{1/2}$ .

$$E = E_{1/2} + \frac{RT}{nF} \ln \frac{i_d - i}{i} \quad \text{Reversible process} \quad (3)$$

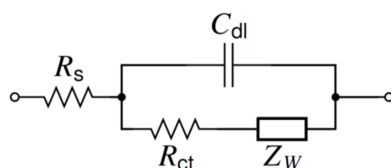
### 2.2. Impedance

#### 2.2.1. General Equations

The Randles circuit (Scheme 1) has been used for the treatment of impedance data [20], where the Warburg element,  $Z_w$ , and Warburg coefficient,  $\sigma$ , are:

$$Z_w = \sigma\omega^{-1/2} - j\sigma\omega^{-1/2} \quad (4)$$

$$\sigma = \frac{RT}{n^2F^2A\sqrt{2}} \left( \frac{1}{D_O^{1/2}C_O^*} + \frac{1}{D_R^{1/2}C_R^*} \right) \quad (5)$$



**Scheme 1.** Randles circuit:  $Z_w$  is the Warburg element,  $R_{ct}$  is the charge transfer resistance,  $R_s$  is the electrolyte resistance (ohmic resistance) and  $C_{dl}$  is the capacitance of the double layer.

The impedance data were analyzed by fitting them to the expressions valid in the case of Randles behavior [21,22], giving the values of the Warburg coefficient,  $\sigma$ , the charge transfer resistance,  $R_{ct}$ , the irreversibility quotient,  $p' = R_{ct}/\sigma$ , and the capacitance of the double layer,  $C_{dl}$ .

#### 2.2.2. Other Treatments

Additionally, other equations can be used to obtain parameter values. When a Nernstian behavior (reversibility) is considered, Equation (6) can be applied.

$$p' = \frac{\sqrt{2D_O}}{K[1 + \exp \epsilon]} \quad (6)$$

$$\text{where } \epsilon = \frac{nF}{RT} (E - E_{1/2}^r) \quad (7)$$

This equation enables calculation of the velocity constant,  $K$  (which, in fact, is the apparent velocity constant,  $K_{ap}$ ), if  $E_{1/2}^r$  and  $D_O$  are known.

The plot of  $p'$  vs.  $E$  present a maximum at

$$E_{max} = E_{1/2}^r + \frac{RT}{nF} \ln\left(\frac{\alpha}{1-\alpha}\right) \quad (8)$$

$$p'_{max} = \sqrt{2D_O} \frac{1-\alpha}{K} \quad (9)$$

These equations enable calculation of the transfer coefficient,  $\alpha$ , and  $K$ . If  $E_{max} < E_{1/2}^r$ , then  $\alpha < 0.5$ .

For the Warburg coefficient, in the minimum in the plot  $\sigma$  vs.  $E$ , we obtain

$$E_m = E^f + \frac{RT}{nF} \ln \sqrt{\frac{D_R}{D_O}} = E_{1/2}^r \quad (10)$$

$$\sigma_m = \frac{4RT}{n^2F^2(C_O^*\sqrt{2D_O} + C_R^*\sqrt{2D_R})} \quad (11)$$

where  $C_O^*$  and  $C_R^*$  are the concentrations of the species  $O$  and  $R$  in the bulk and  $E^f$  is the formal potential. Equation (10) simplifies when  $C_R^* = 0$ . These equations enable the determination of  $E_{1/2}^r$  and  $D_O$ .

The plot of  $R_{ct}$  presents a minimum at

$$E_m = E_{1/2}^r + \frac{RT}{nF} \ln\left(\frac{1-\alpha}{\alpha}\right) \quad (12)$$

$$R_{ctm} = \frac{RTD_O^{1/2}}{n^2F^2(C_O^*\sqrt{D_O} + C_R^*\sqrt{D_R})K(1-\alpha)} \quad (13)$$

If  $E_m > E_{1/2}^r$ , then  $\alpha < 0.5$ .

### 2.3. Kinetic Parameters

To obtain the velocity constant  $K = K_{ap}$ , which is the apparent velocity constant ( $K$  indicates, in our case, the forward velocity constant for the reduction process  $Cd^{2+} + 2e^- = Cd$ ), the following equations can be applied:

$$p' = \frac{\sqrt{2D_O}}{K} (1 + e^\epsilon)^{-1} \quad (14)$$

$$R_{ct} = \frac{RT}{n^2F^2} \frac{1 + e^{-\epsilon}}{C_O^*K} \quad (15)$$

$$K = K_s \exp\left(-\alpha \frac{nF}{RT} (E - E^f)\right) \quad (16)$$

#### 2.3.1. The Influence of the Double Layer (Adsorption)

It is possible to study the influence of the adsorption and the double-layer effects on the kinetic process of  $Cd(II)$  reduction. The values of  $\Phi_2$ , potential at the diffuse layer, and the values of adsorption of TEA and electrode coverage obtained in a previous study [10,11] can be applied here with the corresponding equations.

The following equation represents the Frumkin correction

$$\ln K_t = \ln K_{ap} + \frac{2F}{RT} \varphi_r \quad (17)$$

$$K_t = K_s \exp\left(-\alpha \frac{nF}{RT} (E - E^f - \Phi_r)\right) \quad (18)$$

where  $K_{ap}$  is the apparent velocity constant at which values can be obtained through the impedance analysis (through  $p'$  parameter),  $K_t$  is the corrected velocity constant, or true velocity constant, and  $\Phi_r$  can be calculated as  $\Phi_2$ . Once  $K_t$  is obtained, we can plot  $\ln K_t$  vs.  $E - \Phi_r$  and test the model.

### 2.3.2. Coverage

When adsorbed species are present that influence the electron transfer, some expressions relate the rate constant with the surface coverage [11,17]:

$$K = {}_0K(1 - \theta) + {}_1K\theta \quad (19)$$

$$K = {}_0K(1 - \theta) \exp(A\theta) \quad (20)$$

$$K = {}_0K(1 - \theta)^a \quad (21)$$

$$K = {}_0K \exp(B\theta) \quad (22)$$

where  ${}_0K$  is the rate constant at null surface coverage ( $\theta = 0$ ) and  ${}_1K$  is the rate constant at full surface coverage ( $\theta = 1$ ). These expressions are usually applied in the logarithmic form in order to create linear dependences. In these equations,  $K$  is the apparent rate constant,  $K_{ap}$ , or the true rate constant,  $K_v$  or  $K_t$ , according to previous equations.

## 3. Material and Methods

Measurements were performed in a three-electrode cell. The working electrode (WE) was a DME (see ref. [20] for general details); the counter electrode (CE) was a pool of mercury; and the reference electrode (RE) was a sodium-saturated calomel electrode (SSCE or NaSCE) connected to the cell via a salt bridge filled with the supporting electrolyte. The temperature was  $25 \pm 0.1$  °C. Solutions were prepared from twice-distilled water and analytical-grade chemicals. The supporting electrolyte was perchloric acid maintained at constant activity  $a_{\pm} = 0.418$  ( $c \approx 0.55$  m), according to previous thermodynamic studies on the activity coefficients of perchloric acid and TEA perchlorate mixtures [10,18,19]. The concentrations of TEA perchlorate were 0, 0.75, 2, 5, 10 and 20 mM, but the results for the 20 mM concentration are only taken as a qualitative indication due to their significant dispersion.

Before measurements, oxygen was removed by bubbling argon through the cell. The dc and ac measurements were performed at 1.5 mM Cd(II) concentration (as CdSO<sub>4</sub>) and at 4 s after the mercury drop birth. A new drop was used for each measurement. The Hg mass drop is indicated in Table 1. For these measurements, the network analyzer system described earlier [23,24] was used. The cell impedance was analyzed in the frequency range of 80–10,000 Hz at 5 mV intervals of the dc potential within the Faradaic region. The dc polarograms were also obtained at 5 mV intervals.

**Table 1.** Ilkovic equation (Equations (1) and (2)) with  $n = 2$ ,  $c = 1.5$  mM,  $t = 4$  s.

c(TEA) (mM)	0	0.75	2	5
m (mg)	4.258	4.324	4.196	4.179
$i_d$ ( $\mu$ A)	7.1	7.1	6.7	6.7
$D \times 10^6$ (cm <sup>2</sup> /s)	12.6	12.6	11.4	11.4
Corr sphericity $D \times 10^6$ (cm <sup>2</sup> /s)	9.1	9.1	8.3	8.3

## 4. Results and Discussion

### 4.1. DC Measurements

The polarographic curve for the solution without TEA (Figure 1) shows a reversible reduction of the Cd(II) ions. The half-wave potential is  $E_{1/2}^r = -575$  mV (vs. SSCE), with a value only slightly more negative than that of  $E_{1/2}^r$  reported for other perchlorate media:

the value of  $E_{1/2}^r = -570$  mV (vs. SSCE) in 0.8 M NaClO<sub>4</sub> was reported by [8,9], and the value of  $E_{1/2}^r = -567$  mV or  $-569$  mV (vs. SSCE) in 0.5 M NaClO<sub>4</sub> + 0.5 M HClO<sub>4</sub> medium is reported in the bibliography. Figure 2 plots  $\log(i/(i_d - i))$  vs.  $E$ . The slope of  $\log(i/(i_d - i))$  vs.  $E$  is  $0.033 \text{ mV}^{-1} = 33 \text{ V}^{-1}$ , practically the value of the reversible case ( $nF/(2.3RT)$ , see Equation (3)). The diffusion coefficients for Cd(II) obtained from the Ilkovic equation (Equation (1)) and considering the correction of sphericity (Equation (2)) are  $12.6$  and  $9.1 \times 10^{-6} \text{ cm}^2 \cdot \text{s}^{-1}$ , respectively (see Table 1). These coefficients were also obtained from ac measurements.

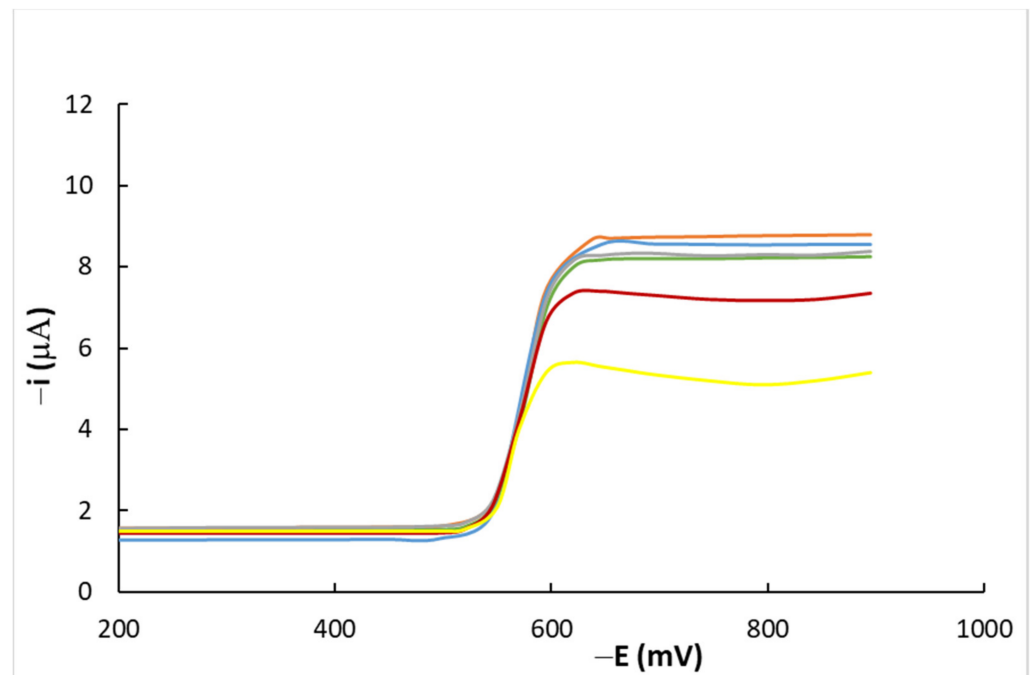


**Figure 1.** Polarograms for Cd(II) in the presence of TEA in 0.55 M perchloric acid solutions. TEA concentrations (mM): 0 (orange), 0.75 (blue), 2 (green), 5 (grey), 10 (red), 20 (yellow).

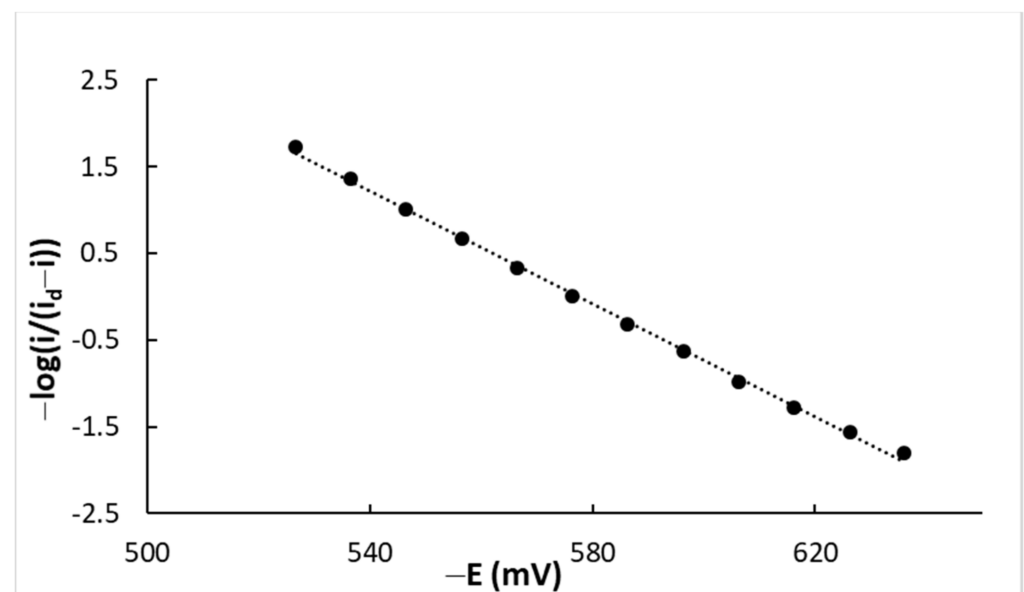


**Figure 2.** Plot of  $\log(i/(i_d - i))$  vs.  $E$  for Cd(II) in 0.55 M perchloric acid solution.

The values of  $D_O$  obtained with the Ilkovic equation are higher than those reported in the bibliography (even the experimental conditions of the concentration and electrolyte

are different), but the latter are more similar to the value of  $D_O$  obtained with the equation that considers the sphericity correction. As we will see later, the value of  $D_O$  obtained with the equation that considers the sphericity correction also agrees better with the value obtained from impedance analysis. The values of  $D_O$  reported in the bibliography are  $8.0 \times 10^{-6} \text{ cm}^2 \cdot \text{s}^{-1}$  in 0.8–1 M  $\text{NaClO}_4$  medium [8,9], and  $7.0$  (or  $8.0$ )  $\times 10^{-6} \text{ cm}^2 \cdot \text{s}^{-1}$  in 0.5 M  $\text{NaClO}_4 + 0.5 \text{ M HClO}_4$  medium.

The solution containing the lowest TEA concentration showed the same polarographic results as the solution without TEA. When the TEA concentration increased, the half-wave potential remained practically the same, although a small decrease was observed in the limit current. For the highest TEA concentrations, the polarographic wave resolved in two sections (Figure 1), showing a maximum and a minimum in the transition from the first wave to the second. The second wave extended to more negative potentials. The current after the first wave when TEA concentration was 20 mM was half of the limit current of the overall process, which seemed to indicate a process involving two electrons, and that the second discharge was inhibited or delayed by TEA. The existence of a “maximum” could be explained because the TEA cations adsorb strongly at negative charges of the electrode [9], and at high TEA concentrations and negative charges of the electrode, TEA cations tend to form an adsorbed monolayer.

The observed influence of the TEA adsorption on the one-step process  $\text{Eu(III)} \rightarrow \text{Eu(II)}$  [11,17] was to shift the polarographic waves to more negative potentials. This reduction is considered to present a mechanism of “outer sphere”. The reduction of  $\text{Cd(II)}$  occurs in a multiple-step process, and the adsorption could influence each step in different ways. For  $\text{Cd(II)}$  reduction in the presence of sucrose, a strong influence in the chemical step and in the first electron transfer was observed at low sucrose concentrations.

#### 4.2. AC Measurements

The impedance or admittance data were analyzed by fitting to the expressions valid in the case of Randles behavior [21,22] giving the values of the Warburg coefficient,  $\sigma$ , resistance to the charge transfer,  $R_{ct}$ , the irreversibility quotient,  $p'$ , and double-layer capacitance,  $C_{dl}$ , at different dc potentials. These values are plotted in Figures 3 and 4 and Figures S1 and S2 (in the Supplementary Information).

From the minimum in the plot of the Warburg coefficient values vs.  $E$  (Figure 3) and from Equations (9) and (10) [22], we can obtain  $E_{1/2}^r$  and  $D_O$ . The results for the different solutions are in Table 2. For all solutions except those with high TEA concentration, we see that  $E_{1/2}^r = -573 \text{ mV}$ , and this value is close to that obtained from polarography ( $-575 \text{ mV}$ ). The value obtained for  $D_O$  was  $9\text{--}10 \times 10^{-6} \text{ cm}^2 \cdot \text{s}^{-1}$ . If we take the value in the minimum of  $\sigma_m = 40 \Omega \cdot \text{s}^{-1/2}$ , with  $n = 2$  and  $c = 1.5 \times 10^{-6} \text{ mol} \cdot \text{cm}^{-3}$ , we thus obtain  $D_O = 9.8 \times 10^{-6} \text{ cm}^2 \cdot \text{s}^{-1}$ .

**Table 2.** Different parameter values from  $\sigma - E$  plots, and in the minimum (m).

$C_{\text{TEA}}/\text{mM}$	0	0.75	2	5	10
$-E_m = -E_{1/2}^r/\text{mV}$	573.0	572.9	573.4	572.4	570.5
$\sigma_m/\Omega \cdot \text{s}^{-1/2}$	39.9	39.0	41.6	41.4	46.8
$D_O \times 10^6/\text{cm}^2 \cdot \text{s}^{-1}$	9.9	10.4	9.1	9.2	7.2
$-E^f/\text{mV}$	573	573	574	573	573

From the value of  $D_R = 10.7 \times 10^{-6} \text{ cm}^2 \cdot \text{s}^{-1}$  in a mercury amalgam [25], the formal potential could be calculated (see Equation (9)); the value  $E^f = -573 \text{ mV}$  is in good agreement with the bibliographic values for perchlorate media (the values of  $E^f = -572 \text{ mV}$  (vs. SSCE) in 0.8 M  $\text{NaClO}_4$  [9], and that of  $-570 \text{ mV}$  vs. SSCE in 1 M  $\text{NaClO}_4$  was also reported [8]). The decrease in the  $D_O$  for TEA concentrations of 2 and 5 mM could be an effect of the TEA cation, because this phenomenon has also been observed for the reduction of  $\text{Eu(III)}$  [17], but the value for the TEA concentrations of 10 mM is not realistic and corresponds to the effect of the adsorption on the electrode discharge, already seen in the polarographic waves.

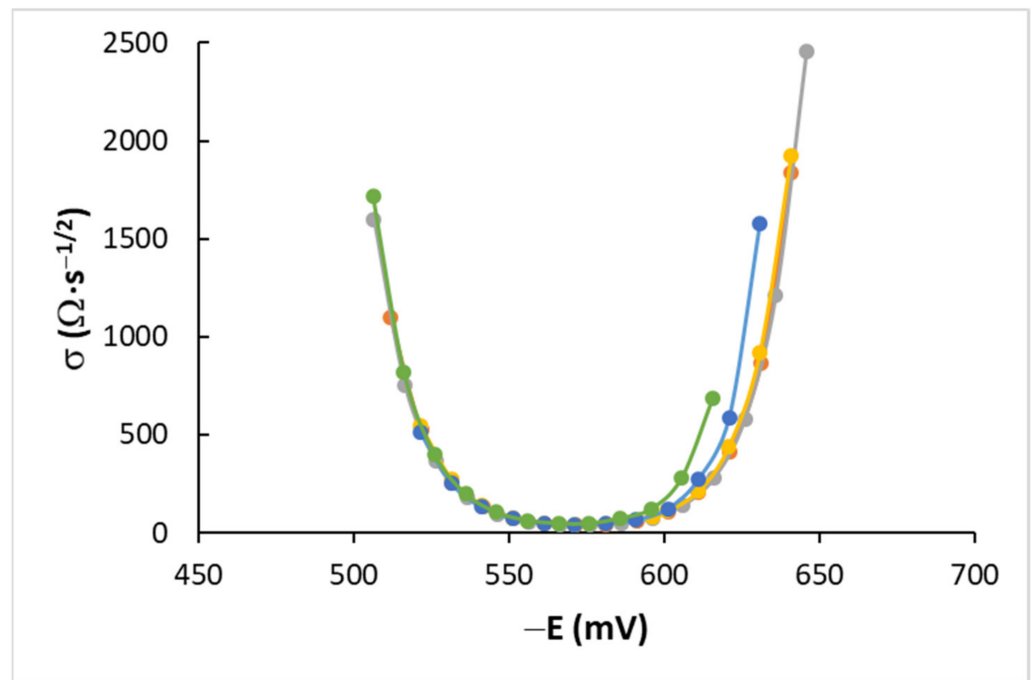


**Figure 3.** Plot of the Warburg coefficient  $\sigma$  vs.  $E$  at different TEA concentrations. TEA concentrations (mM): 0 (orange), 0.75 (grey), 2 (yellow), 5 (blue), 10 (green).

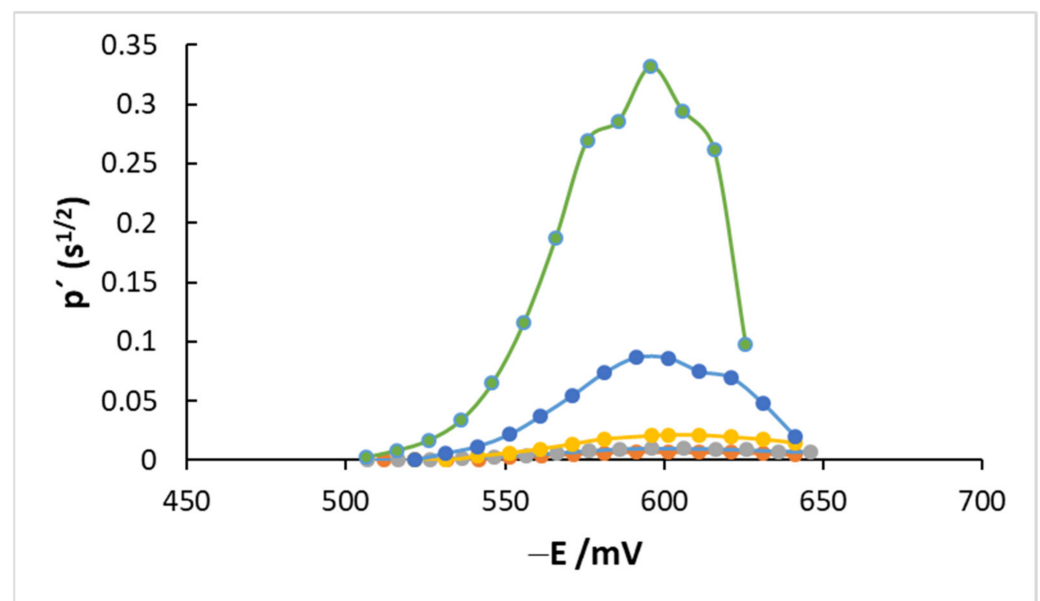


**Figure 4.** Plot of the irreversibility quotient  $p'$  vs.  $E$  at different TEA concentrations. TEA concentrations (mM): 0 (orange), 0.75 (grey), 2 (yellow), 5 (blue), 10 (green).

From the expression of  $p'$  (Equation (6)), we can see that the plot of  $p'$  vs.  $E$  (Figure 4) presents a maximum, predicted by Equations (7) and (8). Table 3 presents the values of  $p'$  at the maximum. The maximum of  $p'$  is shifted to more negative potentials, which means, according to Equation (7), that  $\alpha < 0.5$ . From Equation (7) and  $E_{1/2}^f$ , we obtain  $\alpha_{ap} = 0.11$ , and from Equation (6), values of  $K$  can be obtained. In Table 3, the values of  $K$  at the formal potential are shown ( $K^f$ ). Values of  $\alpha$  between 0.1 and 0.25 in perchlorate medium have been reported, but in some cases, values of  $\alpha = 0$  or 0.68 have also been reported.

**Table 3.** Different parameter values from the plots  $p' - E$ , and in the maximum (max).

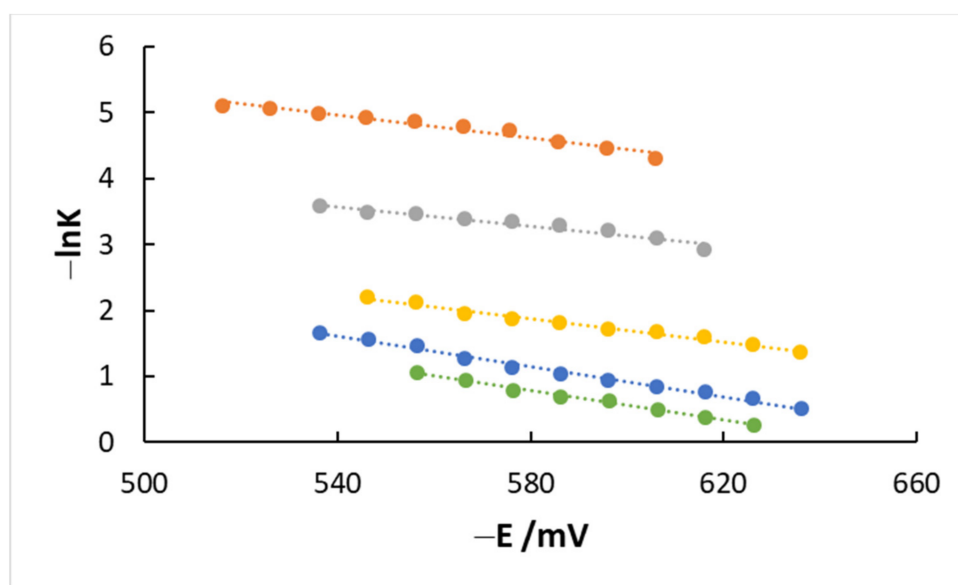
$C_{TEA}/mM$	0	0.75	2	5	10
$-E_{max}/mV$	598.1	600.4	604.5	598.4	593.0
$p'_{max} \times 10^3/s^{1/2}$	7.0	9.9	21.5	88.7	317.0
$K^f/cm \cdot s^{-1}$	0.57	0.40	0.19	0.045	0.013

$K^f$  is calculated from  $p'_{max}$  (Equation (8)), taking  $Do = 10 \times 10^{-6} \text{ cm}^2 \cdot \text{s}^{-1}$  and  $\alpha = 0.11$ . The value of  $\alpha$  is obtained from Equation (7) with  $E_{max} = -600.0 \text{ mV}$  and taking  $E_{1/2}^r = -573.0 \text{ mV}$ .  $K^f$  is an apparent constant.

The plot of  $R_{ct}$  vs.  $E$  (Figure S1) does not show a clear minimum, and for that was not used. This indicates that  $\alpha$  will present a low value, in agreement with the value found previously. Figure S2 plots the values of  $C_{dl}$  versus  $E$ . There is some influence of the frequency of the determination of the differential capacity ( $C_{dl}$ ), which has not been discussed here

The shape of the  $\sigma - E$  and  $p' - E$  plots agrees with the quasi-reversible character of the process, indicated by previously observing the polarographic curves. This reversible character points to large enough values for the velocity constant,  $K$ . From the analysis of the values of the Randles circuit parameters, electrode kinetic parameters, as the velocity constant  $K$ , can be obtained at different potentials (see Equations (13) and (14)).

From the slope in the plot of  $\ln K$  vs.  $E$  (see Equation (15) and Figure 5), we can also obtain the values of  $\alpha_{ap}$ . A linear relationship only holds for the low TEA concentrations within a range of potentials. The obtained value agrees with that indicated before. When the TEA concentration increases, the value of  $\alpha$  becomes more potential-dependent. The slopes are higher at the more negative potentials, indicating an increase in the  $\alpha$  value. A plot of  $\ln K$  vs.  $E$  will be curved in the case of a linear mechanism with more than one rate-determining step.

**Figure 5.** Plot of  $-\ln K$  (obtained from  $p'$  values) vs.  $E$  at different TEA concentrations (mM): 0 (green), 0.75 (blue), 2 (yellow), 5 (grey), 10 (orange).

When the effects of the double layer are considered through  $\Phi_2$ , the values of  $K_t$  can be obtained, according to Equation (16). Thus, the values of  $K_t$  can be related to the surface coverage, according to Equations (18)–(21). Figure 6 plots  $\ln K_t$  vs.  $E - \Phi_2$ . The value of  $\alpha$  obtained from this plot is 0.15, very close to that of 0.11 obtained above. The value of  $\alpha$  in a multi-step mechanism, if  $n = 2$  and CEE mechanism for example, can be 0, 0.25 or 0.75,

depending on the rate controlling step, or taking values in between if there is more than one rate-determining step.

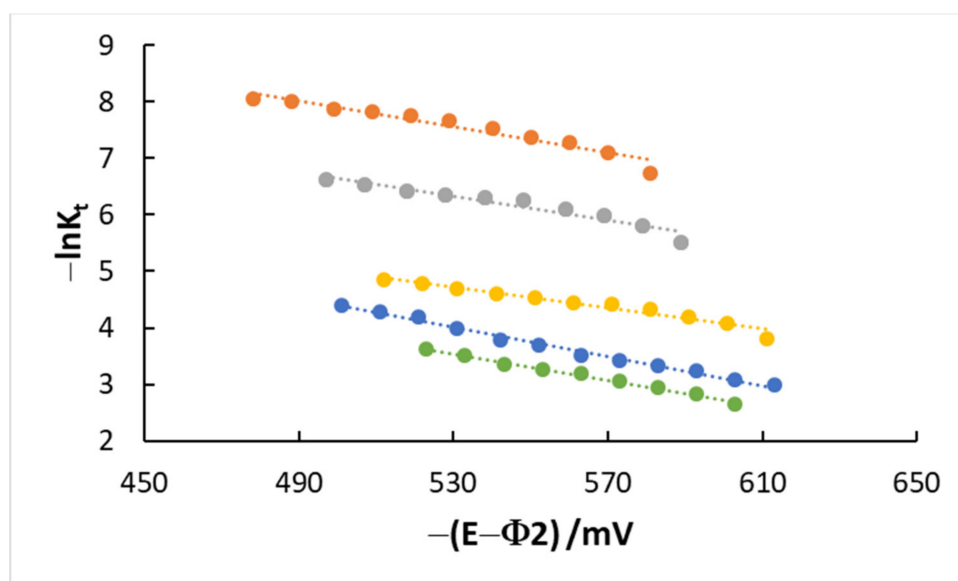


**Figure 6.** Plot of  $-\ln K_t$  vs.  $E - \Phi_2$  at different TEA concentrations (mM): 0 (green), 0.75 (blue), 2 (yellow), 5 (grey), 10 (orange).

#### 4.3. Kinetics and Coverage

The effect of TEA electrode coverage on the velocity constants of the reduction of Cd(II) has been analyzed using several isotherms (Equations (18)–(21)). The adsorption and coverage results were obtained previously [10,11]. The analysis has been performed at several values of  $E - \Phi_2$  in order to consider effects of the double layer (Figure S3, in the Supplementary Information, plots the values of coverage at several values of  $E - \Phi_2$ ). The best fit for the whole coverage range was obtained using Equation (20), with a value of the parameter  $a$  close to 3 (see Figure 7). This indicates an effect of the TEA coverage; a value  $a > 1$  indicates not only a blocking by the physical space occupied by TEA molecules but an electrostatic repulsion between positive ions.

It is also of interest to show other fits. A fit with Equation (21) presented two zones, as did the fit of Equation (19) (see Figure 8). Equation (19) separated the blocking effect by space  $(1 - \theta)$  from the repulsive interaction by the exponential term on  $\theta$  ( $\exp(A\theta)$ ). This could indicate a greater effect of the repulsive interactions at higher coverages, whereas at low coverages, the repulsive interaction would be compensated by the adsorption of perchlorate anions, of opposite charge. This suggests that perhaps a better analysis should include the total adsorption, which is that of a TEA cation plus that of a perchlorate anion (see ref. [10]).

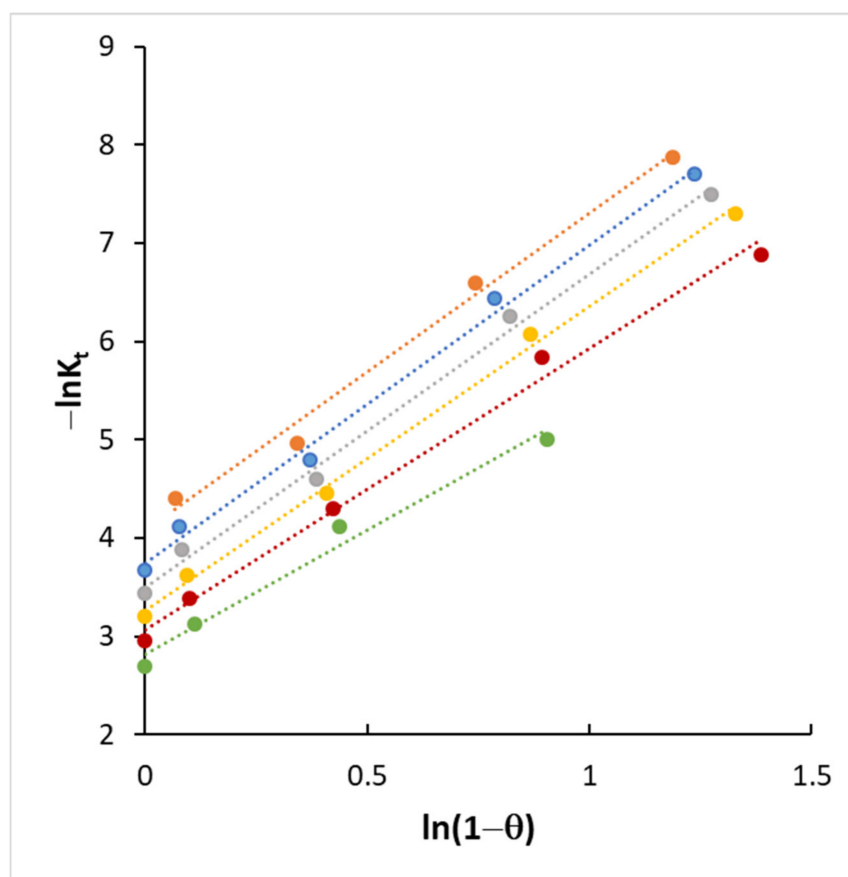


**Figure 7.** Plot of  $-\ln K_t$  vs.  $\ln(1 - \theta)$ , for different values of  $E - \Phi_2$  (mV):  $-500$  (orange),  $-520$  (blue),  $-540$  (grey),  $-560$  (yellow),  $-580$  (red),  $-600$  (green).

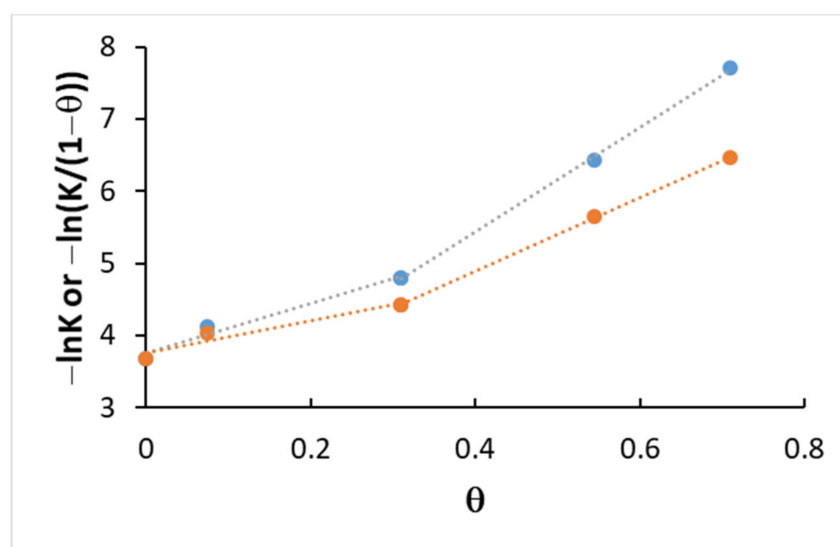


**Figure 8.** Plot of  $-\ln K$  vs.  $\theta$  (blue) and plot of  $-\ln(K/(1 - \theta))$  vs.  $\theta$  (orange), at  $E - \Phi_2 = -520$  mV.

## 5. Conclusions

The existence of two waves in polarograms when the TEA concentration is high, with the second wave shifted to more negative potentials, indicates that a strong TEA adsorption inhibits the second electron transfer. A big change on the surface coverage,  $\theta$ , at low TEA concentrations provokes little change in the current intensity. A slight change

in the adsorption at high TEA concentrations provokes a strong change in the current intensity. Thus, it seems that adsorption especially effects the second electron transfer.

Values of  $E_{1/2}$  and  $D_O$  obtained from both dc and ac measurements agree. The velocity constants showed a decrease as TEA concentration increased, with values ranging from 0.6 to  $0.01 \text{ cm}\cdot\text{s}^{-1}$ . The change in the value of  $\alpha$  ( $\alpha_{ap}$  is potential-dependent) could indicate that the adsorption of TEA changes the mechanism or perhaps influences the electron transfer energy.

Testing the relationship between electrode coverage and velocity constant using several isotherm equations shows that the best fit is obtained with the equation  $K = {}_0K(1 - \theta)^a$ , with an  $a$  value close to three, indicating a blocking effect and electrostatic repulsion due to the TEA cation.

**Supplementary Materials:** The following are available online at <https://www.mdpi.com/article/10.3390/electrochem2030027/s1>, Figure S1: Plot of the charge transfer resistance  $R_{ct}$  vs.  $E$  at different TEA concentrations. TEA concentrations (mM): 0 (orange), 0.75 (grey), 2 (yellow), 5 (blue), 10 (green). Figure S2: Plot of the double-layer capacitance  $C_{dl}$  vs.  $E$  at different TEA concentrations. TEA concentrations (mM): 0 (orange), 0.75 (grey), 2 (yellow), 5 (blue), 10 (green). Figure S3: Coverage  $\theta$  vs.  $(E - \Phi_2)$  at different TEA concentrations (mM): 0.75 (orange), 2 (grey), 5 (yellow), 10 (blue).

**Funding:** This research received no external funding.

**Institutional Review Board Statement:** Not applicable.

**Informed Consent Statement:** Not applicable.

**Data Availability Statement:** Data available in a publicly accessible repository.

**Conflicts of Interest:** The author declares no conflict of interest.

## References

1. Struijs, J.; Sluyters-Rehbach, M.; Sluyters, J.H. The mechanism of the Cd(II) reduction in 1 M fluoride, perchlorate and chloride solutions at the DME, a combined DC, AC admittance and demodulation study. *J. Electroanal. Chem.* **1984**, *171*, 177–193. [CrossRef]
2. Bongenaar, C.P.M.; Remijnse, A.G.; Sluyters-Rehbach, M.; Sluyters, J.H. On the selection of the most probable mechanism of the Cd(II) reduction at mercury from 1M KF solution. *J. Electroanal. Chem.* **1980**, *111*, 139–153. [CrossRef]
3. Bongenaar, C.P.M.; Remijnse, A.G.; Temmerman, E.; Sluyters-Rehbach, M.; Sluyters, J.H. A faradaic impedance study of the electrochemical reduction of Cd(II) ions from aqueous 1M (KF+KCl) mixed electrolyte solution at the dropping mercury electrode. *J. Electroanal. Chem.* **1980**, *111*, 155–162. [CrossRef]
4. Brug, G.J.; Sluyters-Rehbach, M.; Sluyters, J.H. A study of the reduction of tris-oxalato Fe(III) from aqueous 1 M oxalate solution at a polycrystalline gold electrode. *J. Electroanal. Chem.* **1984**, *176*, 297–308. [CrossRef]
5. Souto, R.M.; Sluyters-Rehbach, M.; Sluyters, J.H. On the catalytic effect of thiourea on the electrode reduction of cadmium (II) ions at the DME from aqueous 1 M KF solutions. *J. Electroanal. Chem.* **1986**, *201*, 33–45. [CrossRef]
6. Sluyters-Rehbach, M.; Souto, R.M.; Sluyters, J.H. Induced reactant adsorption accompanying the reduction of cadmium(II) ions from 1 M KF solutions containing thiourea at elevated concentrations: An ac admittance study. *J. Electroanal. Chem.* **1989**, *264*, 195–215. [CrossRef]
7. Souto, R.M.; Saakes, M.; Sluyters-Rehbach, M.; Sluyters, J.H. The catalysis of the electrochemical reduction of cadmium ions by chloride ions. A mechanistic study in mixed 1 M KF + KCl aqueous solutions at the dropping mercury electrode. *J. Electroanal. Chem.* **1987**, *245*, 167–189. [CrossRef]
8. Saakes, M.; Sluyters-Rehbach, M.; Sluyters, J.H. The inhibition of Cd(II) reduction at the DME from aqueous 1 M NaClO<sub>4</sub> by sucrose. *J. Electroanal. Chem.* **1990**, *282*, 161–174. [CrossRef]
9. Saakes, M.; Sluyters-Rehbach, M.; Souto, R.M.; Sluyters, J.H. The reduction pathway of the Cd(II) reduction in mixed (0.8-x) M NaClO<sub>4</sub> + x M NaF base electrolytes. *J. Electroanal. Chem.* **1989**, *264*, 217–234. [CrossRef]
10. Torrent, J.; González, R.; Sanz, F.; Molero, M. The adsorption of tetraethylammonium ions at a mercury electrode from perchlorate solutions. *J. Electroanal. Chem.* **1989**, *270*, 381–393. [CrossRef]
11. Torrent, J. Estudi Termodinamic de L'adsorcio en les Interfaces Hg/HClO<sub>4</sub> i Hg/HClO<sub>4</sub>, TEAClO<sub>4</sub> (aq). Influencia Sobre la Reduccio de l'Eu(III). Ph.D. Thesis, University of Barcelona, Barcelona, Spain, 1988.
12. Vallés, E.; Sanz, F.; Virgili, J. Efecto de algunos cationes tetraalquilamonio sobre la cinética electrodica Eu(III)/Eu(II) a recubrimientos intermedios. *An. Quim.* **1985**, *81A*, 233–240.
13. Devanathan, M.A.V.; Fernando, M.J. Specific adsorption of tetra-alkyl-ammonium iodides at the mercury-water interface and the structure of the electrical double layer. *Trans. Faraday Soc.* **1962**, *58*, 368–381. [CrossRef]

14. Piro, J.; Bennes, R.; Bou Karam, E. Étude de l'adsorption des ammoniums quaternaires à l'interface mercure-solution par mesures des charges de l'électrode. *J. Electroanal. Chem.* **1974**, *57*, 399–412. [[CrossRef](#)]
15. Kimmerle, F.M.; Ménard, H. Ionic surface excesses of the tetramethylammonium halides. *J. Electroanal. Chem.* **1974**, *54*, 101–121. [[CrossRef](#)]
16. Hamdi, M.; Bennes, R.; Schuhmann, D.; Vanel, P. A study of superficial associations at a mercury electrode in the case of tetrabutylammonium halide solutions. *J. Electroanal. Chem.* **1980**, *108*, 255–270. [[CrossRef](#)]
17. Torrent, J.; Sanz, F. Influencia de la adsorción del catión tetraetilamonio en la reducción del europio(III). *An. Quim.* **1991**, *87*, 327–331.
18. Torrent, J.; Sanz, F.; Virgili, J. Activity coefficients of aqueous perchloric acid. *J. Solut. Chem.* **1986**, *15*, 363–375. [[CrossRef](#)]
19. Torrent, J.; Sanz, F. Activity coefficients of tetraethylammonium perchlorate in aqueous solutions. *Port. Electrochim. Acta* **1986**, *4*, 51–59.
20. Bard, A.J.; Faulkner, L.R. *Electrochemical Methods. Fundamentals and Applications*; John Wiley & Sons: Hoboken, NJ, USA, 1980.
21. Sluyters-Rehbach, M.; Sluyters, J.H. Sine Wave Methods in the Study of Electrode Processes. In *Electroanalytical Chemistry*; Bard, A.J., Ed.; Marcel Dekker: New York, NY, USA, 1970; Volume 4, pp. 1–128.
22. Sluyters-Rehbach, M.; Sluyters, J.H. AC Techniques. In *Comprehensive Treatise of Electrochemistry*; Bockris, J.O., Conway, B.E., Yeager, E., White, R.E., Eds.; Plenum Press: New York, NY, USA, 1984; Volume 9, pp. 177–292.
23. Bongenaar, C.P.M.; Sluyters-Rehbach, M.; Sluyters, J.H. A high-precision network analyzer system for the measurement of the electrode impedance of both stationary and non-stationary electrode, with special attention to the dropping mercury electrode. *J. Electroanal. Chem.* **1980**, *109*, 23–39. [[CrossRef](#)]
24. Brug, G.J.; van den Eeden, A.L.G.; Sluyters-Rehbach, M.; Sluyters, J.H. The analysis of electrode impedances complicated by the presence of a constant phase element. *J. Electroanal. Chem.* **1984**, *176*, 275–295. [[CrossRef](#)]
25. Van der Pool, F.; Sluyters-Rehbach, M.; Sluyters, J.H. On the elucidation of mechanisms of electrode reactions by combination of AC and faradaic rectification polarography. Application to the  $Zn^{2+}/Zn(Hg)$  and  $Cd^{2+}/Cd(Hg)$  reduction. *J. Electroanal. Chem.* **1975**, *58*, 177–188. [[CrossRef](#)]